IEEE Access
Multidisciplinary | Rapid Review | Open Access Journal

Received August 28, 2018, accepted October 9, 2018, date of publication October 15, 2018, date of current version November 9, 2018.

Digital Object Identifier 10.1109/ACCESS.2018.2875822

Direct Position Determination of Non-Circular Sources Based on a Doppler-Extended Aperture With a Moving Coprime Array

YAN-KUI ZHANG, HAI-YUN XU, BIN BA, DA-MING WANG, AND WEI GENG
National Digital Switching System Engineering and Technological Research Center, Zhengzhou 450000, China
Corresponding author: Yan-Kui Zhang (zhang yk 2018@163.com)

This work was supported by the National Natural Science Foundation of China under Grant 61401513.

ABSTRACT Direct position determination (DPD) is a new promising technique in wireless location. Compared with conventional two-step localization methods, DPD achieves a higher accuracy by directly estimating the source location without computing the intermediate parameters. However, all the existing angle-based DPD algorithms for non-circular sources use uniform linear arrays, which lead to low degrees of freedom and poor estimation precision, and do not make use of the Doppler characteristics of the moving station. To improve the DPD performance, this paper proposes a novel DPD algorithm for non-circular sources based on a Doppler-extended aperture with a moving coprime array. First, the coprime array is introduced to angle-based DPD, and an extended array model is established by exploiting the Doppler characteristics of the moving array. The characteristics of non-circular sources are used to further improve the positioning accuracy. Finally, merging the subspace data for each measuring position, the target positions can be obtained. The Cramer–Rao lower bound of the DPD algorithm is presented for non-circular sources in a coprime array combined with Doppler-extended aperture. Performance analysis and the simulation experiments show that compared with the conventional two-step localization method and DPD based on a uniform array, including subspace data fusion and weighted subspace fitting algorithms, the proposed algorithm effectively improves the location accuracy at the expense of a slight complexity increase and can determine the location of multiple targets in underdetermined conditions.

INDEX TERMS Direct position determination (DPD), coprime array, non-circular source, Doppler shift, Cramer Rao lower bound (CRLB).

I. INTRODUCTION

Wireless location technology is an important research topic in array signal processing. It is widely used in intelligent transportation, logistics management, industry 4.0 and so on [1]. There are currently two kinds of passive wireless location technologies: two-step positioning technologies and direct position determination (DPD) technologies. Two-step technologies first estimate the location parameters of the target sources, including the transmission delay, the angle of arrival and the Doppler frequency shift, and then calculate the position coordinates of the target sources from their geometric relationships [2]–[4]. DPD is based on two-step positioning, which establishes the cost function directly from the relationship in coordinate geometry between the observation station and the target source positions. The location coordinates of the target sources can be directly determined in one step [5]–[7]. DPD does not require the estimation of intermediate parameters, avoids the accumulation and propagation of errors, and improves the positioning accuracy. It has therefore attracted wide attention from researchers at home and abroad.

DPD technology was first introduced by Weiss [8] in 2004, and it gives the basic model for DPD. Current DPD technologies are divided into single-station DPD and multi-station DPD. Single-station DPD uses the measurement parameters (such as direction-of-arrival, time delay, Doppler information and so on) of the station for each observation position [9]–[11]. Single-station DPD is widely applied because of its simple structure, low complexity, low cost and requirement of no synchronization. The single-station DPD technique was proposed by the German researcher Demissie [12] in 2008. It gives the DPD model for a single

moving station based on the direction-of-arrival, and presents a solution to the subspace data fusion (SDF) algorithm. Based on this model, Oispuu and Nickel [13] improved on SDF by combined the maximum likelihood (ML) method and Capon iterative optimization to increase the positioning accuracy. Doppler information is employed to make full use of the characteristics of the moving array [14], [15], and weight subspace fitting (WSF) and maximum likelihood (ML) algorithms are used to further improve the positioning precision.

Circular sources (CS) and non-circular sources (NS) refer to sources whose elliptical covariance is zeros and nonzero, respectively. There are many non-circular sources in modern communications systems, including binary phase shift keying (BPSK) and M-ary amplitude shift keying (MASK) modulation signals. Researchers have carried out research into DPD by making full use of the characteristics of non-circular sources. A DPD technique is proposed in a moving array [16] that uses the characteristics of NS to improve the positioning accuracy, and derived the Cramer-Rao lower bound (CRLB) of this model. Current research into DPD focuses mainly on the uniform linear array, which has limited degrees of freedom (DOF) and the estimation accuracy. New coprime arrays, a kind of non-uniform sparse arrays, have appeared in recent years and they can obtain bigger array apertures, insignificant coupling effects, a higher DOF and higher estimation accuracy [17]–[23], because the sensor spacing is greater than half the wavelength. To date, there have been no researches on DPD techniques based on coprime arrays. In practice, we should not only consider the overdetermined conditions but also the underdetermined conditions, where the former is the number of sensors in the array is larger than the number of sources while the latter is smaller. To expand the aperture of the DPD with a moving array to its full extent, improve the estimation accuracy and estimate the signal position under underdetermined conditions effectively, this paper introduces the coprime array into DPD based on the angle for non-circular sources with a moving array. The estimation accuracy is improved by making full use of the large array aperture and high DOF characteristics. At the same time, this paper uses the Doppler information to full advantage, and uses the Kronecker product to expand the array aperture. The positioning accuracy is greatly improved, and effective estimation of multiple sources in the underdetermined condition can finally be achieved.

The main contributions of this paper are listed as follows:

1) DPD is applied to coprime array for the first time. The DPD model, extended from a uniform array to a sparse non-uniform array, has effectively improved the location accuracy and enables to estimate multiple non-circular sources effectively.

2) Doppler information is introduced, which greatly expands the array aperture, increases the DOF and improves the estimation accuracy. The algorithm proposed in this paper can achieve effective positioning in underdetermined conditions.

3) CRLB is derived for the proposed model, demonstrating that proposed model can achieve a significant decrease in the variance of the position estimation. The paper also presents a detailed complexity analysis and simulation experiments.

The remainder of the paper is arranged as follows. Section 2 introduces the DPD model with a moving array. Section 3 describes the design of the DPD for non-circular sources based on a Doppler-extended aperture with a moving coprime array, and derives the CRLB of the proposed model. Section 4 presents a complexity analysis and the results of performance simulation experiments, thus validating our algorithm. Section 5 presents our conclusions.

II. DPD MODEL WITH A MOVING ARRAY

A. NOTATION CONVENTIONS

Notations used in this paper are as follows:

- $\mathbf{I}_N$ denotes the N dimensional unit array.
- $(\bullet)^*$, $(\bullet)^{\mathrm{T}}$ and $(\bullet)^{\mathrm{H}}$ respectively denote the conjugate, transposition and conjugate transpose.
- $\bigcup$ stands for the union.
- $\otimes$ is the Kronecker product.
- $E(\bullet)$ represents the mathematical expectation.
- Re $[\bullet]$ and Im $[\bullet]$ represent the real and imaginary parts.

B. DPD MODEL WITH A MOVING ARRAY

We assume that there are D stationary uncorrelated narrowband targets impinging to the measuring station, and the corresponding location of the target source is $\mathbf{p}_i = (x_i, y_i)^{\mathrm{T}}$, $i \in \{1, 2, \cdots D\}$. Thus, the location vector of all source targets can be expressed as $\mathbf{p} = \left(\mathbf{p}_1^{\mathrm{T}}, \mathbf{p}_2^{\mathrm{T}} \cdots \mathbf{p}_D^{\mathrm{T}}\right)^{\mathrm{T}}$. The receiving array at the observation station uses a coprime array with M sensors. Depending on the characteristics of the array, the underdetermined condition is when $D < M$, that is the number of sources is less than the number of array sensors; the overdetermined condition is when $D \geq M$. The observation station is moved to L positions during the measurement, where the observation position is $\mathbf{u}_l = (x_l, y_l)^{\mathrm{T}}$ and the number of snapshot at each observation position is K. The velocity of the observation station is $\mathbf{v}$. Geometry of one moving antenna array and multiple transmitters is shown in Fig. 1.

If we denote the kth sending snapshot at the lth observation location for the ith source by $s_{l,i}(k)$, and $\mathbf{s}_l(k)$ is the kth sending snapshot at the lth observation location for D sources, then

$$\mathbf{s}_l(k) = \left[s_{l,1}(k)\ s_{l,2}(k)\ \cdots\ s_{l,D}(k)\right]^{\mathrm{T}} \tag{1}$$

If we assume that the noise is additive Gaussian white noise, the kth received snapshot signal at the lth observation location can be expressed as

$$\mathbf{r}_l(k) = \sum_{i=1}^{D} \mathbf{a}\left(\theta_{l,i}\right) s_{l,i}(k) + \mathbf{n}_l(k) \tag{2}$$

where the steering vector is

$$\mathbf{a}\left(\theta_{l,i}\right) = \left[1, \mathrm{e}^{-j2\pi d \cos\theta_{l,i}/\lambda}, \cdots, \mathrm{e}^{-j2\pi(M-1)d\cos\theta_{l,i}/\lambda}\right]^{\mathrm{T}} \tag{3}$$

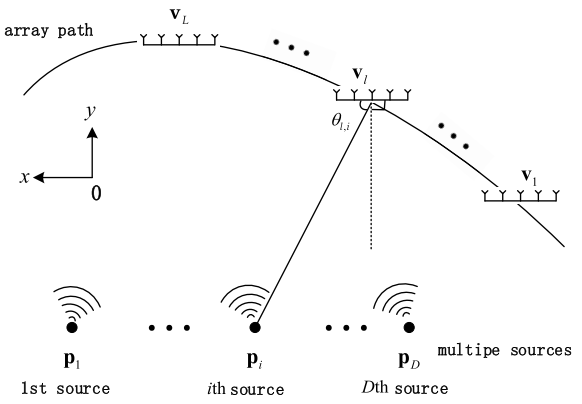

FIGURE 1. Geometry of one moving antenna array and multiple transmitters.

where d is the array sensor spacing. We usually take half of the signal wavelength, and so $d = \lambda/2$. $\theta_{l,i}$ denotes azimuth of the ith source impinging to the lth observation position, whose cosine $\cos\theta_{l,i}$ has the similar format as the estimation of two-step location. The array can be equivalent to a point when the distance between the target and the array is far enough (much greater than array aperture). Thus, $\theta_{l,i}$ can be represented directly by the geometric relationship in DPD as

$$\theta_{l,i} = \arccos\frac{\Delta x_{l,i}}{|\Delta_{l,i}|} = \arccos\frac{(x_i - x_l)}{|(x_i - x_l, y_i - y_l)|} \tag{4}$$

III. DPD OF NON-CIRCULAR SOURCES BASED ON A DOPPLER-EXTENDED APERTURE WITH A MOVING COPRIME ARRAY (NDMCA-DPD)

A. NDMCA-DPD

The DPD model with a moving array was introduced in the previous section. The model based on the uniform linear array has the small array aperture. This section introduces the coprime array into the DPD model and uses the Doppler characteristics to expand the array aperture. We know that each subarray of coprime array has the sensor spacing greater than half the wavelength and then a "pseudo peak" will appear because of the array manifold has a periodicity of 2π and the position between the pseudo peak and the true peak is related to the sensor spacing. When the sensor spacings of two subarrays are coprime integer multiples of half the wavelength, the position of the true peak can be overlapped and the pseudo peak is removed.

Fig. 2 illustrates the coprime array model, where $d = \lambda/2$ and λ is the wavelength of impinging signal. Subarray 1 has N sensors and subarray 2 has M sensors, where N and M are coprime integers. Correspondingly, the sensor spacings of two subarray are Md and Nd, respectively. The subarrays coincide at the first sensor, so the total number of sensors is $M + N - 1$. Considering the Doppler characteristics of the above array, the kth receiving snapshot of the lth observation position is expressed as

$$\mathbf{r}_l(k) = \sum_{i=1}^{D} \breve{\mathbf{a}}_l(\mathbf{p}_i)\, s_{l,i}(k)\, e^{j2\pi f_l(\mathbf{p}_i)kT_s} + \mathbf{n}_l(k) \tag{5}$$

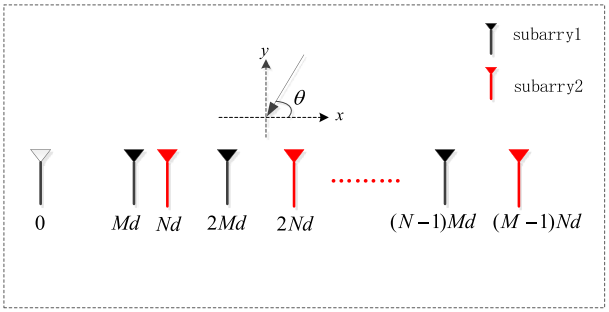

FIGURE 2. Geometry of coprime array.

Introduction of the coprime linear array has changed the array manifold, so the steering vector is

$$\breve{\mathbf{a}}_l(\mathbf{p}_i) = \left[1, \cdots, e^{-\frac{j2\pi d_{M+N-1}(x_l - x_i)/\lambda}{|(x_l - x_i, y_l - y_i)|}}\right]^{\mathrm{T}} \tag{6}$$

The location d_j of the jth array sensor is given by

$$d_j \in \{0, Md \cdots M(N-1)d\} \bigcup \{Nd \cdots N(M-1)d\} \tag{7}$$

T_s in (5) represents the sampling interval for each observation position. The Doppler shift at the lth position $f_l(\mathbf{p}_i)$ represent the frequency offset due to the movement of the observation position, and is given by

$$f_l(\mathbf{p}_i) = f_c \frac{\mathbf{v}_l^{\mathrm{T}}(\mathbf{p}_i - \mathbf{u}_l)}{c\,\|\mathbf{p}_i - \mathbf{u}_l\|} \tag{8}$$

$$\mathbf{r}_l(k) = \mathbf{B}_l(\mathbf{p})\,\mathbf{s}_l(k) + \mathbf{n}_l(k) \tag{9}$$

where the array manifold $\mathbf{B}_l(\mathbf{p})$ is given by

$$\mathbf{B}_l(\mathbf{p}) = \left[\mathbf{b}_l(\mathbf{p}_1) \cdots \mathbf{b}_l(\mathbf{p}_D)\right] \tag{10}$$

$$\mathbf{b}_l(\mathbf{p}_i) = \mathbf{g}_l(\mathbf{p}_i) \otimes \breve{\mathbf{a}}_l(\mathbf{p}_i) \tag{11}$$

$$\mathbf{g}_l(\mathbf{p}_i) = \left[1, e^{j2\pi f_l(\mathbf{p}_i)T_s}, \cdots, e^{j2\pi f_l(\mathbf{p}_i)(K-1)T_s}\right]^{\mathrm{T}} \tag{12}$$

As the transmitted signal phase for the same signal source is fixed in non-circular signals, we have

$$s_{l,i}(k) = s_{l,0}^{(i)}(k)\, e^{j\varphi_i} \tag{13}$$

where $s_{l,0}^{(i)}(k)$ is a real value representing the signal amplitude andφ_i indicates the ith phase of the transmitted signal. Thus, we can write

$$\mathbf{s}_l(k) = \begin{bmatrix} s_{l,1}(k) \\ s_{l,2}(k) \\ \vdots \\ s_{l,D}(k) \end{bmatrix} = \begin{bmatrix} s_{l,0}^{(1)}(k)\, e^{j\varphi_1} \\ s_{l,0}^{(2)}(k)\, e^{j\varphi_2} \\ \vdots \\ s_{l,0}^{(D)}(k)\, e^{j\varphi_D} \end{bmatrix}$$

$$= \begin{bmatrix} e^{j\varphi_1} & 0 & \cdots & 0 \\ 0 & e^{j\varphi_2} & \ddots & \vdots \\ \vdots & \ddots & \ddots & 0 \\ 0 & \cdots & 0 & e^{j\varphi_D} \end{bmatrix} \begin{bmatrix} s_{l,0}^{(1)}(k) \\ s_{l,0}^{(2)}(k) \\ \vdots \\ s_{l,0}^{(D)}(k) \end{bmatrix} = \Phi \mathbf{s}_{l,0}(k) \tag{14}$$

$$\Phi = \begin{bmatrix} e^{j\varphi_1} & 0 & \cdots & 0 \\ 0 & e^{j\varphi_2} & \ddots & \vdots \\ \vdots & \ddots & \ddots & 0 \\ 0 & \cdots & 0 & e^{j\varphi_D} \end{bmatrix} \tag{15}$$

$$\mathbf{s}_{l,0}(k) = \left[s_{l,0}^{(1)}(k)\ s_{l,0}^{(2)}(k)\ \cdots\ s_{l,0}^{(D)}(k) \right]^{\mathrm{T}} \tag{16}$$

where $\mathbf{s}_{l,0}(k)$ is a real vector. From these expressions, we can restructure the received signal using (9)

$$\mathbf{z}_l(k) = \begin{bmatrix} \mathbf{r}_l(k) \\ \mathbf{r}_l^*(k) \end{bmatrix} = \begin{bmatrix} \mathbf{B}_l(\mathbf{p})\,\mathbf{s}_l(k) \\ \mathbf{B}_l^*(\mathbf{p})\,\mathbf{s}_l^*(k) \end{bmatrix} + \begin{bmatrix} \mathbf{n}_l(k) \\ \mathbf{n}_l^*(k) \end{bmatrix} \tag{17}$$

as

$$\mathbf{s}_l^*(k) = \Phi^* \mathbf{s}_{l0}^*(k) = \Phi^* \Phi^{-1} \mathbf{s}_l(k) = \left(\Phi^*\right)^2 \mathbf{s}_l(k) \tag{18}$$

So (19) is equivalent to the following form

$$\begin{aligned} \mathbf{z}_l(k) &= \begin{bmatrix} \mathbf{r}_l(k) \\ \mathbf{r}_l^*(k) \end{bmatrix} = \begin{bmatrix} \mathbf{B}_l(\mathbf{p}) \\ \mathbf{B}_l^*(\mathbf{p})\,\Phi^*\Phi^* \end{bmatrix} \mathbf{s}_l(k) + \begin{bmatrix} \mathbf{n}_l(k) \\ \mathbf{n}_l^*(k) \end{bmatrix} \\ &= \mathbf{H}_l(\mathbf{p})\,\mathbf{s}_l(k) + \begin{bmatrix} \mathbf{n}_l(k) \\ \mathbf{n}_l^*(k) \end{bmatrix} \end{aligned} \tag{19}$$

where

$$\begin{aligned} \mathbf{H}_l(\mathbf{p}) &= \begin{bmatrix} \mathbf{B}_l(\mathbf{p}) \\ \mathbf{B}_l^*(\mathbf{p})\,\Phi^*\Phi^* \end{bmatrix} \\ &= \left[\mathbf{h}_l(\mathbf{p}_1)\ \mathbf{h}_l(\mathbf{p}_2)\ \cdots\ \mathbf{h}_l(\mathbf{p}_D) \right] \end{aligned} \tag{20}$$

$$\mathbf{h}_l(\mathbf{p}_i) = \begin{bmatrix} \mathbf{a}_l(\mathbf{p}_i) \\ \mathbf{a}_l^*(\mathbf{p}_i)\,\mathrm{e}^{-\mathrm{j}2\varphi_i} \end{bmatrix} \tag{21}$$

Then the covariance matrix of received signals for each measurement position is calculated, and eigenvalue decomposition (EVD) is performed as follows:

$$\begin{aligned} \mathbf{R}_l &= \frac{1}{K} \sum_{k=1}^{K} \mathbf{z}_l(k)\,\mathbf{z}_l^{\mathrm{H}}(k) \\ &= \left[\mathbf{U}_l^{(s)}, \mathbf{U}_l^{(n)} \right] \Sigma_l \left[\mathbf{U}_l^{(s)}, \mathbf{U}_l^{(n)} \right]^{\mathrm{H}} \end{aligned} \tag{22}$$

Take $\mathbf{U}_l^{(n)} = \begin{bmatrix} \mathbf{U}_{l,1}^{(n)} \\ \mathbf{U}_{l,2}^{(n)} \end{bmatrix}$, where $\mathbf{U}_{l,1}^{(n)}$ and $\mathbf{U}_{l,2}^{(n)}$ have the same dimensions. From the above deduction,

$$\mathbf{U}_{l,1}^{(n)} = \left(\mathbf{U}_{l,2}^{(n)} \right)^* \tag{23}$$

Moreover, $\left(\mathbf{U}_{l,1}^{(n)} \right)^{\mathrm{T}} = \left(\mathbf{U}_{l,2}^{(n)} \right)^{\mathrm{H}}$, where $\mathbf{U}_{l,2}^{(n)} \left(\mathbf{U}_{l,1}^{(n)} \right)^{\mathrm{H}}$ and $\mathbf{U}_{l,1}^{(n)} \left(\mathbf{U}_{l,2}^{(n)} \right)^{\mathrm{H}}$ are in a conjugate relationship. From the location estimation expressions for non-circular sources in [16], the SDF objective function for non-circular sources can be obtained as

$$\begin{aligned} f(\mathbf{p}) = \sum_{l=1}^{L} \Bigg\{ & \mathbf{h}_l^{\mathrm{H}}(\mathbf{p})\,\mathbf{U}_{l,1}^{(n)} \left(\mathbf{U}_{l,1}^{(n)} \right)^{\mathrm{H}} \mathbf{h}_l(\mathbf{p}) \\ & - \left| \mathbf{h}_l^{\mathrm{T}}(\mathbf{p})\,\mathbf{U}_{l,2}^{(n)} \left(\mathbf{U}_{l,1}^{(n)} \right)^{\mathrm{H}} \mathbf{h}_l(\mathbf{p}) \right| \Bigg\} \end{aligned} \tag{24}$$

The target source locations can be obtained through a spectral peak search of minimum points.

B. SUMMARY OF ALGORITHM STEPS

Based on the above analysis, steps of NDMCA-DPD can be summarized as follows:

Algorithm 1 Algorithm Steps of NDMCA-DPD

1. Construct a DPD model considering (2) and Fig. 1 with a single moving array .

2. Use (11) to extend the dimension of the receiving array by the Doppler shift of the observation station, and calculate the extended covariance matrix $\mathbf{R}_l$. Obtain the noise subspace $\mathbf{U}_l^{(n)}$ by performing EVD on the extended receiving signal covariance matrix.

3. Decompose and reconstruct the eigenvalues in the noise subspace and use (25) to construct the cost function of the source coordinates.

4. Solve the cost function (25) by searching for the spectral peaks, where the D minimum values of the spectral peaks are the location coordinates of the target sources.

C. CRLB OF NDMCA-DPD

The CRLB as the lower bound of the unbiased estimation variance represents the degree of location estimation deviation. CRLB of steps of NDMCA-DPD is quoted from [24]–[27]. First, containing all observation locations, the received signal snapshot vector is

$$\mathbf{z}(k) = \left[\mathbf{z}_1^{\mathrm{T}}(k), \cdots \mathbf{z}_L^{\mathrm{T}}(k) \right]^{\mathrm{T}} \tag{25}$$

The corresponding transmission signal vector and the noise vector can be expressed as $\mathbf{s}(k)$ and $\mathbf{n}(k)$. Assuming that noise follows a Gaussian distribution, then

$$\mathbf{s}(k) = \left[\mathbf{s}_1^{\mathrm{T}}(k), \cdots \mathbf{s}_L^{\mathrm{T}}(k) \right]^{\mathrm{T}} \tag{26}$$

$$\mathbf{n}(k) = \mathbf{z}(k) - \mathbf{H}\mathbf{s}(k) \tag{27}$$

$$\begin{aligned} P(\mathbf{z}(1) \cdots, \mathbf{z}(K)) = & \frac{1}{(2\pi)^{(M+N-1)K} \left(\sigma_n^2/2\right)^{(M+N-1)K}} \\ & \times \exp - \frac{1}{\sigma_n^2} \sum_{k=1}^{K} [\mathbf{z}(k) - \mathbf{H}\mathbf{s}(k)]^{\mathrm{H}} \\ & \times [\mathbf{z}(k) - \mathbf{H}\mathbf{s}(k)] \end{aligned} \tag{28}$$

where the array manifold $\mathbf{H}$ is

$$\mathbf{H} = \begin{bmatrix} \mathbf{H}_1(\mathbf{p}) & \cdots & \mathbf{0} \\ \vdots & \ddots & \vdots \\ \mathbf{0} & \cdots & \mathbf{H}_L(\mathbf{p}) \end{bmatrix} \tag{29}$$

The logarithm likelihood function can be obtained by taking the logarithm of (28)

$$\begin{aligned} \mathbf{L}(\mathbf{z}(1), \cdots, \mathbf{z}(K)) = & -(M+N-1) \\ & \times K \left[\ln(2\pi) - \ln\left(\sigma_n^2/2\right) \right] \\ & - \frac{1}{\sigma_n^2} \sum_{k=1}^{K} [\mathbf{z}(k) - \mathbf{H}\mathbf{s}(k)]^{\mathrm{H}} [\mathbf{z}(k) - \mathbf{H}\mathbf{s}(k)] \end{aligned} \tag{30}$$

Define $\bar{\mathbf{s}}_k = \mathrm{Re}[\mathbf{s}(k)]$ and $\tilde{\mathbf{s}}_k = \mathrm{Im}[\mathbf{s}(k)]$. The Fisher information matrix $\Omega = [E(\chi\chi^{\mathrm{T}})]^{-1}$, where

$$\chi^{\mathrm{T}} = \partial \mathbf{L}/\partial\left[\sigma_n^2, \bar{\mathbf{s}}^{\mathrm{T}}(1), \tilde{\mathbf{s}}^{\mathrm{T}}(1) \cdots, \bar{\mathbf{s}}^{\mathrm{T}}(K), \tilde{\mathbf{s}}^{\mathrm{T}}(K), \mathbf{p}^{\mathrm{T}}\right] \tag{31}$$

Finally, the Cramer Rao lower bound expression for non-circular sources can be obtained from the Fisher information matrix

$$CRLB(\mathbf{p}) = \frac{\sigma_n^2}{2}\left\{\sum_{k=1}^{K} \mathrm{Re}\left[\mathbf{F}^{\mathrm{H}}(k)\mathbf{D}^{\mathrm{H}}\mathbf{P}_{\mathbf{H}}^{\perp}\mathbf{D}\mathbf{F}(k)\right]\right\}^{-1} \tag{32}$$

where $\mathbf{P}_{\mathbf{H}}^{\perp} = \mathbf{I} - \mathbf{P}_{\mathbf{H}} = \mathbf{I} - \mathbf{H}(\mathbf{H}^{\mathrm{H}}\mathbf{H})^{-1}\mathbf{H}^{\mathrm{H}}$, $\mathbf{F}(k) = \mathbf{I}_2 \otimes diag(\mathbf{s}(k))$, $\mathbf{I}_2 = \begin{bmatrix} 1 & 0 \\ 0 & 1 \end{bmatrix}$, $\mathbf{D} = \left[\frac{\partial \mathbf{H}^{\mathrm{H}}}{\partial x_1}, \frac{\partial \mathbf{H}^{\mathrm{H}}}{\partial y_1}, \cdots, \frac{\partial \mathbf{H}^{\mathrm{H}}}{\partial x_D}, \frac{\partial \mathbf{H}^{\mathrm{H}}}{\partial y_D}\right]$.

IV. PERFORMANCE ANALYSIS

A. COMPLEXITY ANALYSIS

In this section, we compare the proposed algorithm with the two-step positioning algorithm, SDF algorithm and WSF algorithm. The number of array sensors is $M + N - 1$. For convenience of expression, define $N_{\mathrm{a}} = M + N - 1$. The number of snapshots is K, the number of sources is D. J_x, J_y and $J_\theta$represent the number of search grids for the x coordinates, the y coordinates and the angle. The computational complexity of the algorithm consists of three main parts: while calculating the expanded covariance matrix $\mathbf{R}_l$ at each observation location, the computational complexity is $O(4LK^2N_a^2)$; while carrying out eigenvalue decomposition for the above covariance matrix, the computational complexity is $O(8LK^3N_a^3)$; while decomposing the noise subspace, constructing the cost function of DPD for non-circular sources and searching for the spectrum peaks, the computational complexity is $O(2J_xJ_yKN_a(KN_a - D))$. Thus the computational complexity of this paper is $O(8LK^3N_a^3 + (4L + 2J_xJ_y)K^2N_a^2 - 2J_xJ_yDKN_a)$. The complexity of the two-step positioning algorithm, the SDF algorithm and the WSF algorithm are given in Table 1.

TABLE 1. Comparison of algorithm complexity

Algorithm	Complexity
Proposed	$O(8LK^3N_a^3 + (4L + 2J_xJ_y)K^2N_a^2 - 2J_xJ_yDKN_a)$
Two-step	$O(LN_a^3 + (LK + J_\theta)N_a^2 - J_\theta DN_a + LDJ_xJ_y)$
SDF	$O(LN_a^3 + (LK + J_xJ_y)N_a^2 - J_xJ_yDN_a)$
WSF	$O(L(1 + J_xJ_y)K^3N_a^3 + LK^2N_a^2 + LD^3)$

Table 1 shows that the two-step positioning method reduces the two-dimensional coordinates search to doing a one-dimensional DOA search twice, and the computational complexity is the lowest. The complexity of this paper is slightly higher than that of the SDF algorithm (see [13]) and the two-step localization algorithm (this method divides the positioning process into two parts: parameter estimation and location calculation), which is lower than the WSF algorithm (see [15]). Under the same conditions, compared with the two-step location algorithm, the increase in complexity mainly comes from the expanded array aperture required by the non-circular characteristics of the source. At the same time, compared with the SDF algorithm, the increase in complexity mainly comes from the expanded array manifold resulting from full use of the Doppler information. The complexity of the four algorithms is shown in Fig. 3 when J_x, J_y and J_θ take the same value and change from 1000 to 10000, $M = 4$, $N = 5$, $K = 20$,and the number of sources $D = 2$.

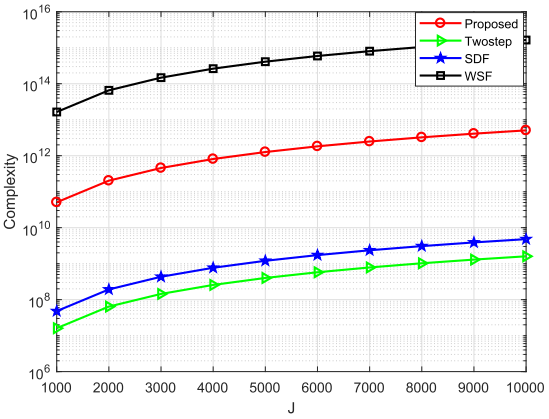

FIGURE 3. Computation complexity with the number of search grid.

B. SIMULATION RESULTS

This paper proposes a DPD method for non-circular sources based on a Doppler-extended aperture with a moving coprime array. We assumed that the noise is Gaussian white noise in all simulation experiments. To verify the estimation performance of this algorithm, we applied Monte Carlo experiments to compare the estimation performance with the performance of the two-step localization algorithm, SDF algorithm and WSF algorithm. The SDF algorithm is based on the subspace algorithm, and the cost function of the location coordinates is established by covering the subspace data for each measurement position. It is a typical direct position determination method based on the angle made with a single moving station [13]. The WSF algorithm is based on the SDF method. It improves the positioning accuracy by replacing the MUSIC method with the weight subspace fitting method, and [15] gives a detailed introduction. To measure the positioning accuracy of this algorithm, we define the root mean square error (RMSE) as

$$\mathrm{RMSE} = \sqrt{\frac{1}{QD}\sum_{m=1}^{Q}\sum_{i=1}^{D}\left\|\hat{\mathbf{p}}_i(m) - \mathbf{p}_i\right\|^2} \tag{33}$$

Where Q is the number of Monte Carlo experiments, D is the number of source targets and $\hat{\mathbf{p}}_i(m)$ is the ith source location of the mth Monte Carlo experiment. The simulation parameters are given in Table 2.

TABLE 2. Simulation conditions for the experiments.

Simulation Parameters	Value
Speed of light	$c = 3 \times 10^8 m/s$
Carrier frequency	$f = 2.1GHz$
Number of antennas	$M = 4, N = 5$
Sensor spacing	$M\lambda/2, N\lambda/2$
Numer of sources	$D = 2$
Source locations	$(-1200, 100)$,$(1700, -510)$
Snapshot number	$K = 20$
Observation speed	$\mathbf{v} = (10, 0)\, m/s$
Observation locations	$(-5500, -3000)$,$(-1500, -3000)$, $(1500, -3000)$,$(5500, -3000)$
No. of Monte Carlo experiments	$Q = 200$
Signal to noise ratio(SNR)	$SNR = -10 \sim 20dB$

Simulation 1: Positioning performance of this algorithm for non-circular sources in the underdetermined condition.

To verify the performance of this algorithm in the underdetermined condition at different SNRs, the estimation scatter plot is simulated when the SNR is -10 dB and 20 dB. The number of sources is 9 (the number of array sensors is 8). The estimation results are shown in Fig. 4, Fig. 5 and Fig. 6. The simulation shows that the algorithm can not only estimate the location of all the sources accurately with a high SNR, but can also effectively estimate the source location in the underdetermined condition with a low SNR.

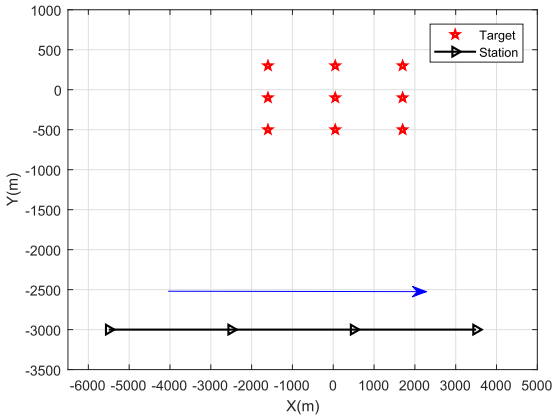

FIGURE 4. Trajectory of the station movement related to the target sources.

Simulation 2: Comparison of the RMSE performance of the proposed algorithm, two-step location algorithm, SDF algorithm, WSF algorithm and the CRLB with different SNRs.

The RMSE performances of the proposed algorithm, two-step algorithm, SDF algorithm and WSF algorithm are simulated with the simulation parameters given in Table 2, and the comparison is shown in Fig. 7. The simulation results show that the performance of DPD is better than the two-step location algorithm. Using the same parameters, the performance of the proposed algorithm is better than the WSF and SDF algorithms. The coprime array and use of the Doppler information significantly extend the array aperture, which effectively improves the estimation accuracy of the algorithm and reduces the CRLB.

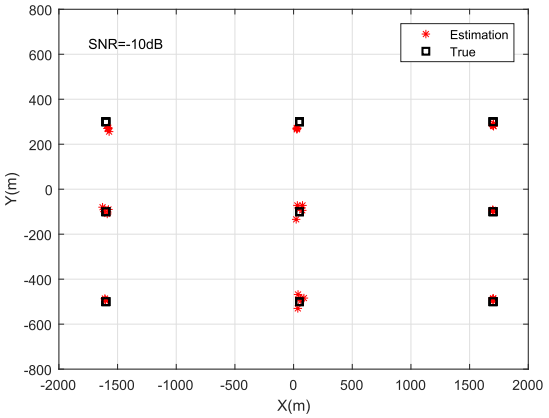

FIGURE 5. Positioning performance of the proposed algorithm (*SNR* = −10dB).

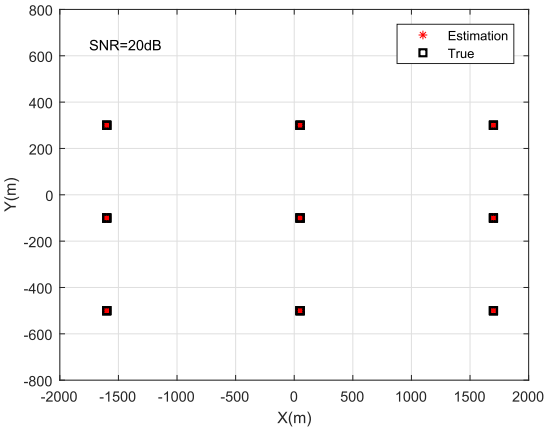

FIGURE 6. Positioning performance of the proposed algorithm (*SNR* = 20dB).

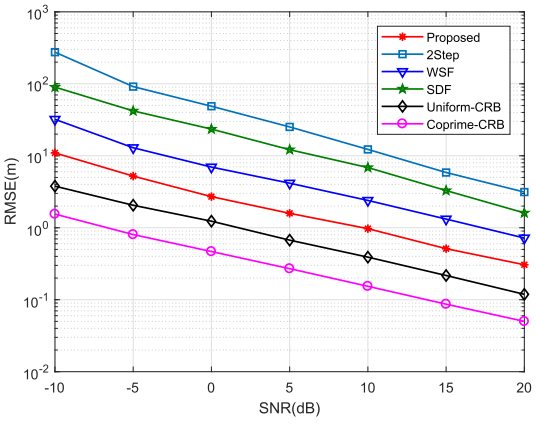

FIGURE 7. RMSE performance comparison of different *SNR*.

Simulation 3: Comparison of the RMSE performance of the proposed algorithm, two-step location algorithm, WSF algorithm, SDF algorithm and the CRLB under different snapshots.

The number of snapshots is an important factor affecting the positioning accuracy. The larger the number of snapshots, the more samples and the longer the signal accumulation time. In this simulation, the number of snapshots is changed from 10 to 600, with SNRs of −10 dB and 20 dB. The other parameters are the same as in Table 2. The RMSE performance under the different snapshots is shown in Fig. 8 and Fig. 9. The figures show that the estimation performance of these algorithms improves with an increased number of snapshots; the DPD performance is better than the performance of the two-step algorithm under the same conditions. The proposed algorithm performs best at the same number of snapshots.

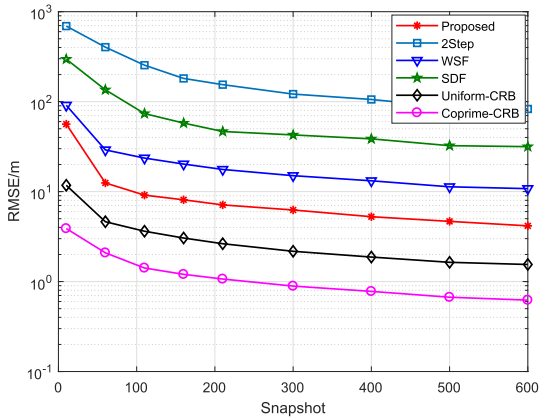

FIGURE 8. RMSE performance comparison of different snapshots(*SNR*=-10dB).

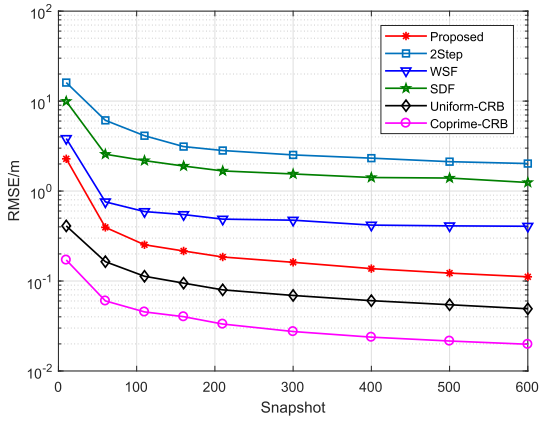

FIGURE 9. RMSE performance comparison of different snapshots(*SNR*=20dB).

V. CONCLUSION

The existing DPD algorithms for non-circular sources are all based on the uniform linear array, which leads to low degrees of freedom and poor estimation precision, and the Doppler characteristics of the moving station are not made use of. To solve this problem, this paper presents a DPD algorithm based on a Doppler-expanded aperture for non-circular sources with a moving coprime array. This algorithm introduces the coprime array into the DPD model, and makes full use of the Doppler information of the observation station, which increases the array aperture and the DOF. The characteristics of non-circular sources are used fully to further improve the positioning accuracy. The complexity analysis and simulation experiments perform that, compared with the two-step positioning algorithm, SDF algorithm and WSF algorithm, the proposed algorithm can not only determine the location of non-circular sources in underdetermined conditions effectively, but can also improve the positioning accuracy with only a slight increase in complexity.

REFERENCES

[1] Z.-L. Dai, W.-J. Cui, B. Ba, and Y.-K. Zhang, "Two-dimensional direction-of-arrival estimation of coherently distributed noncircular signals via symmetric shift invariance," *Acta Phys. Sin.*, vol. 66, no. 22, pp. 701–712, Jun. 2017.

[2] T. Tirer and A. J. Weiss, "Performance Analysis of a High-resolution direct position determination method," *IEEE Trans. Signal Process.*, vol. 65, no. 3, pp. 544–554, Feb. 2017.

[3] J. Li, L. Yang, F. Guo, and W. Jiang, "Coherent summation of multiple short-time signals for direct positioning of a wideband source based on delay and Doppler," *Digit. Signal Process.*, vol. 48, pp. 58–70, Jan. 2016.

[4] L. Zhi-Yu, R. Yan-Qing, B. Bin, W. Da-Ming, and Z. Jie, "An improved direct position determination method based on correlation accumulation of short-time signals with variable velocity receivers," *Acta Phys. Sin*, vol. 66, no. 2, pp. 70–79, Jun. 2017.

[5] W. Xia and W. Liu, "Distributed adaptive direct position determination of emitters in sensor networks," *Signal Process.*, vol. 123, pp. 100–111, Jun. 2016.

[6] L. Tzafri and A. J. Weiss, "High-resolution direct position determination using MVDR," *IEEE Trans. Wireless Commun.*, vol. 15, no. 9, pp. 6449–6461, Sep. 2016.

[7] E. Tzoreff and A. J. Weiss, "Expectation-maximization algorithm for direct position determination," *Signal Process.*, vol. 133, pp. 32–39, Apr. 2016.

[8] A. J. Weiss, "Direct position determination of narrowband radio frequency transmitters," *IEEE Signal Process. Lett.*, vol. 11, no. 5, pp. 513–516, May 2004.

[9] M. Zhang, F. Guo, and Y. Zhou, "A single moving observer direct position determination method using a long baseline interferometer," *Acta Aeronaut. Astronaut. Sin.*, vol. 34, no. 2, pp. 378–386, Feb. 2013.

[10] T. Tirer and A. J. Weiss, "High resolution direct position determination of radio frequency sources," *IEEE Signal Process. Lett.*, vol. 23, no. 2, pp. 192–196, Feb. 2016.

[11] Z. Lu, J. Wang, B. Ba, and D. Wang, "A novel direct position determination algorithm for orthogonal frequency division multiplexing signals based on the time and angle of arrival," *IEEE Access*, vol. 5, pp. 25312–25321, Oct. 2017.

[12] B. Demissie, M. Oispuu, and E. Ruthotto, "Localization of multiple sources with a moving array using subspace data fusion," in *Proc. 11th Int. Conf. Inf. Fusion*, Cologne, Germany, May 2008, pp. 131–137.

[13] M. Oispuu and U. Nickel, "Direct detection and position determination of multiple sources with intermittent emission," *Signal Process.*, vol. 90, no. 12, pp. 3056–3064, Dec. 2010.

[14] Y. L. Wang, Y. Wu, and S. C. Yi, "An efficient direct position determination algorithm combined with time delay and Doppler," *Circuits, Syst., Signal Process*, vol. 35, no. 2, pp. 635–649, Feb. 2016.

[15] J. Yin, D. Wang, Y. Wu, and R. Liu, "Direct localization of multiple stationary narrowband sources based on angle and Doppler," *IEEE Commun. Lett.*, vol. 21, no. 12, pp. 2630–2633, Dec. 2017.

[16] J.-X. Yin, Y. Wu, and D. Wang, "Direct position determination of multiple noncircular sources with a moving array," *Circuits, Syst., Signal Process*, vol. 36, no. 10, pp. 4050–4076, Oct. 2017.

[17] Y. D. Zhang, S. Qin, and M. G. Amin, "DOA estimation exploiting coprime arrays with sparse sensor spacing," in *Proc. ICASSP*, Florence, Italy, May 2014, pp. 2267–2271.

[18] X. Wang, Z. Chen, S. Ren, and S. Cao, "DOA estimation based on the difference and sum coarray for coprime arrays," *Digit. Signal Process.*, vol. 69, pp. 22–31, Oct. 2017.

[19] H. Zhai, X. Zhang, and W. Zheng, "DOA estimation of noncircular signals for coprime linear array via locally reduced-dimensional Capon," *Int. J. Electron.*, vol. 105, no. 5, pp. 709–724, Sep. 2018.
[20] S. Qin, Y. D. Zhang, and M. G. Amin, "Generalized coprime array configurations for direction-of-arrival estimation," *IEEE Trans. Signal Process.*, vol. 63, no. 6, pp. 1377–1390, Mar. 2015.
[21] C. L. Liu and P. P. Vaidyanathan, "Cramér-Rao bounds for coprime and other sparse arrays, which find more sources than sensors," *Digit. Signal Process.*, vol. 61, pp. 43–61, Feb. 2017.
[22] P. Pal and P. P. Vaidyanathan, "Nested arrays: A novel approach to array processing with enhanced degrees of freedom," *IEEE Trans. Signal Process.*, vol. 58, no. 8, pp. 4167–4181, Aug. 2010.
[23] S. Qin, Y. D. Zhang, M. G. Amin, and F. Gini, "Frequency diverse coprime arrays with coprime frequency offsets for multitarget localization," *IEEE J. Sel. Topics Signal Process.*, vol. 11, no. 2, pp. 321–335, Mar. 2017.
[24] B. Bin, L. Guo-Chun, L. Tao, L. Yu-Cheng, and W. Yu, "Joint for time of arrival and direction of arrival estimation algorithm based on the subspace of extended Hadamard product," *Acta Phys. Sin.*, vol. 64, no. 7, pp. 403–411, 2015.
[25] L. Zhang, Q. Huang, and Y. Fang, "Conditional and unconditional CRB of DOA estimation in spherical harmonics domain," in *Proc. ICSP*, Bangkok, Thailand, Mar. 2017, pp. 424–428.
[26] H. Abeida and J. P. Delmas, "Direct derivation of the stochastic CRB of DOA estimation for rectilinear sources," *IEEE Signal Process. Lett.*, vol. 24, no. 10, pp. 1522–1526, Oct. 2017.
[27] P. Stoica and A. Nehorai, "MUSIC, maximum likelihood, and Cramer-Rao bound," *IEEE Trans. Acoust., Speech, Signal Process.*, vol. 37, no. 5, pp. 720–741, May 1989.

YAN-KUI ZHANG was born in 1990. He received the B.S. and M.S. degrees from the National Digital Switching System Engineering and Technological Research Center, Zhengzhou, China, in 2013 and 2016, where he is currently pursuing the Ph.D. degree in communications and information system. His main research interests are in the areas of array signal processing and wireless communication.

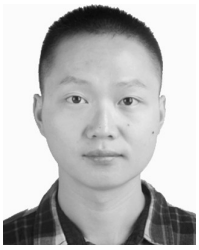

HAI-YUN XU received the B.S. degree from the National Digital Switching System Engineering and Technological Research Center, Zhengzhou, China, in 2016, where he is currently pursuing the M.S. degree in communications and information system. His main research interests are in the areas of wireless communication theory, signal processing, and parameter estimation.

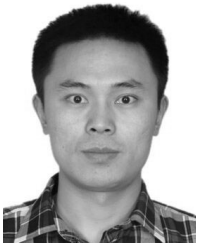

BIN BA was born in 1987. He received the M.S. and Ph.D. degrees from the National Digital Switching System Engineering and Technological Research Center (NDSC), Zhengzhou, China, in 2012 and 2015, respectively. He is currently involved in communications and information system at NDSC. His main research interests are in the areas of wireless communication theory, signal processing, and parameter estimation.

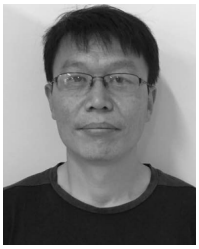

DA-MING WANG was born in 1970. He is currently a Professor with the National Digital Switching System Engineering and Technological Research and Development Center, Henan, China. His main research interests include signal processing and satellite mobile communication.

WEI GENG was born in 1960. She is currently a Research Librarian with the National Digital Switching System Engineering and Technological Research and Development Center, Henan, China. Her main research interest includes intelligent information processing and information research.